THE EFFECT OF TEMPERATURE MODIFICATION ON THE PROPERTIES OF Fe-BASED AMORPHOUS ALLOYS

O. M. Hertsyk[1], T. H. Hula[1], M. O. Kovbuz[1], O. A. Ezers'ka[2], Yu. O. Kulyk[1], N. L. Pandiak[3]
[1] *Ivan Franko National University of Lviv, 6, Kyrylo & Mefodiy St., Lviv, UA–79005, Ukraine,*
[2] *Fraunhofer Institut Fertigungstechnik Materialforschung, Wiener Straße 12, 2835, Bremen, Germany,*
[3] *Ukrainian National Forestry University, 103, General Chuprynka St., Lviv, UA–79057, Ukraine,*
e-mails: o_hertsyk@yahoo.com, djunjer1@gmail.com

(Received 27 March 2022; in final form 01 August 2022; accepted 02 August 2022; published online 01 December 2022)

We investigated the influence of temperature modification on the physicochemical properties of amorphous alloys $Fe_{80}Si_6B_{14}$, $Fe_{78.5}Ni_{1.0}Mo_{0.5}Si_{6,0}B_{14.0}$, $Fe_{73.1}Cu_{1.0}Nb_{3.0}Si_{15.5}B_{7.4}$, $Fe_{51.7}Ni_{21.7}Cr_{6.2}Mo_{0.6}V_{1.5}Si_{5.2}B_{13.1}$ at $T = 77$ K during 0.5, 1.0, 2.0, 3.0 hours, and 7, days and at the temperature range $(273 \div 673)$ K during 1 hour.

After the heat treatment of the amorphous alloys, minor changes in the structure, elemental composition of the surface, and microhardness of materials were observed. The electrochemical characteristics of the samples in the 0.5 M aqueous NaCl solution were determined. The lower corrosion resistance of $Fe_{80}Si_6B_{14}$ alloy and the higher one of $Fe_{51.7}Ni_{21.7}Cr_{6.2}Mo_{0.6}V_{1.5}Si_{5.2}B_{13.1}$ were established. The surface layers that are formed on the surface of a multicomponent amorphous alloy have the highest resistance.

Key words: amorphous metallic alloys, temperature modification, structural characteristics, electrochemical properties.

DOI: https://doi.org/10.30970/jps.26.4801

I. INTRODUCTION

Temperature modification of amorphous metallic alloys (AMA) based on Fe causes changes in their structure and elemental composition, and, therefore, affects the important physicochemical properties of such materials. Depending on the heat treatment mode and elemental composition, Fe-based alloys can undergo various changes. Since amorphous state is metastable, the amorphous alloys transform into a more stable crystalline state upon heating, losing their specific characteristics [1–5] or nanocrystalline, which has special properties [6, 7].

Rapid cooling, which is used in the technology of manufacturing amorphous alloys, inhibits the diffusion process in the solid phase [8]. As a result, amorphous metallic alloys do not have such defects as secondary phases, segregation, which are usually formed due to diffusion during slow cooling. Therefore, AMAs are considered to be ideal chemically homogeneous alloys, especially corrosion resistant and able to withstand extreme conditions.

Complex investigations of amorphous alloys, which were subjected to low-temperature treatment at the temperature of liquid nitrogen [9, 10], showed the absence of significant structural changes. The neutron diffraction method shows that the process of cryotreatment of amorphous magnetic alloys leads to irreversible structural changes in the near order up to 12 Å. As a result of annealing at a temperature of 400°C, the density is redistributed up to 100Å.

The study of the changes that take place in amorphous Fe-based alloys as a result of heat treatment is important for predicting new characteristics and possible further application of alloys.

II. EXPERIMENTAL DETAILS

Experiments were carried out for the following amorphous metallic alloys based on iron: $Fe_{80}Si_6B_{14}$ (AMA-1), $Fe_{78.5}Ni_{1.0}Mo_{0.5}Si_{6.0}B_{14.0}$ (AMA-2); $Fe_{73.1}Cu_{1.0}Nb_{3.0}Si_{15.5}B_{7.4}$ (AMA-3); $Fe_{51.7}Ni_{21.7}Cr_{6.2}Mo_{0.6}V_{1.5}Si_{5.2}B_{13.1}$ (AMA-4) obtained using the melt spinning technique in a helium atmosphere on a copper wheel with a circumferential speed of about 30 m/s. Alloys were obtained in the Kyiv Kurdyumov Institute for Metal Physics of the Ukraine NAS in the form of strips 20–25 μm thick and 1–3 mm wide, respectively. We evaluated the surface activity of the contact (c) and external (e) surfaces of the tape [11].

The heating of the alloy samples was performed in a muffle furnace SNOP-16.2.5./9-H5 at the temperature range $(273 \div 673)$ K. The duration of isothermal treatment was 1 hour. Low-temperature treatment of the AMA samples based on Fe was performed in liquid nitrogen N_2 ($T = 77$ K) during 0.5, 1.0, 2.0, 3.0 hours, and 7 days.

Structural investigations were carried out by X-ray diffraction (XRD) measurements using DRON-3M with the CuK-radiation. The average interatomic distances were determined using the Fourier transformati-

on method [12].

The elemental composition of the experimental samples was investigated by applying energydispersion spectrometer Oxford INCAEnergy 51-ADD0098, part of scanning electron microscope Jeol 7000F.

The PMT-3 device was used to test the microhardness of the AMA samples using Vickers method. A diamond pyramid with an 136° angle was pressed into the test sample under the load. The diagonal of the print was measured with an ocular micrometer. The microhardness number H_ν was calculated using the formula: $H_\nu = k \cdot P/d^2 = 1854 \cdot P/d^2$, $[H_0] = [\mathrm{kg/mm^2}]$, where P is the weight of the load, g; d is the diagonal of the print, μm; k is a coefficient that depends on the shape of the pyramid and is 1854 for the Vickers method [13].

To evaluate the corrosion resistance of amorphous alloys, we used the chronopotentiometric method, which enables one to study spontaneous electrochemical processes running on the electrode–solution boundary according to the changes in the free potential (E). The changes in the free potential of the AMA-electrode were recorded as compared with the changes in the free potential of the Cl^- | AgCl | Ag (sat) electrode. The role of the working electrode was played by an amorphous metallic alloy strip ($s = 0.15$ cm^2) and the duration was 20 min. The initial (E_0) and final (E_f) values of potentials were determined from the dependence $E = f(t)$. The electrochemical investigations were performed by using an IPM PC-R Jaissle Potentiostat/Galvanostat in the 0.5 M aqueous solution of NaCl [14].

The electrochemical impedance spectroscopy (EIS) was carried out using an Autolab®/PGSTAT-20 device equipped with a frequency analyzer and a differential electrometric amplifier (Eco Chemie BV, the Netherlands). The accumulated results were processed by using the Autolab-4.9 software. The impedance components were computed for a circuit containing two resistors and a capacitor ($R_1(Q_\mathrm{dl}R_2)$), where R_1 is the resistance of the electrolyte, the 0.5 M NaCl aqueous solution, R_2 is the charge-transfer resistance, and Q_dl is an element of the constant phase characterizing the capacitance of the double layer [15]. Also, we determined the reliability coefficient α and surface roughness R_f.

III. RESULTS AND DISCUSSIONS

Evaluation of the temperature modification effect on physicochemical properties is important for AMA samples that have a wide range of applications in extreme conditions [16].

The X-ray study and analysis of the obtained values of short-range parameters determined from the scattering intensity curves $I(s)$ of AMA $Fe_{78.5}Ni_{1.0}Mo_{0.5}Si_{6.0}B_{14.0}$, pre-treated in the temperature range $(293 \div 673)$ K and 77 K (Fig. 1, Tables 1, 2) found a slight dependence of structural parameters on temperature. For the initial sample, the average interatomic distance $r_1 = 0.253$ nm is close to the sum of two atomic radii of Fe ($r_\mathrm{Fe} = 0.127$ nm), which indicates the dominant influence of microgroups of the α-Fe in the formation of the short-range order in amorphous alloy $Fe_{78.5}Ni_{1.0}Mo_{0.5}Si_{6.0}B_{14.0}$ (Table 1). After the low-temperature treatment of AMA samples system Fe–Si–B–(Me), there are also no significant changes in the structure (Table 2), which indicates the durability of such materials to heat treatment at the above temperatures.

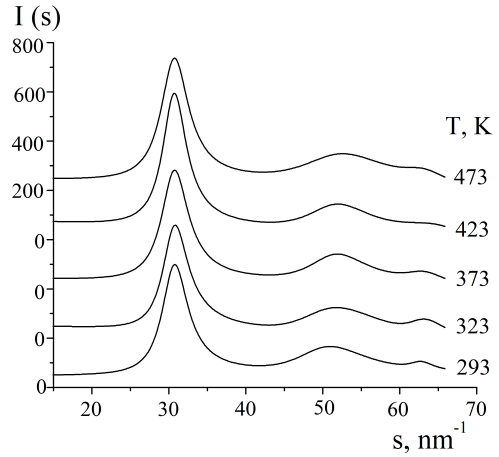

Fig. 1. Scattering intensity curves of AMA $Fe_{78.5}Ni_{1.0}Mo_{0.5}Si_{6.0}B_{14.0}$

T, K	s_1, nm^{-1}	r_1, nm	$a(s_1)$
293	30.6	0.253	3.14
373	30.5	0.256	3.29
473	31.0	0.254	2.98
573	30.8	0.255	3.15
673	30.6	0.257	3.16

Table 1. Structural characteristics of AMA $Fe_{78.5}Ni_{1.0}Mo_{0.5}Si_6B_{14}$ after heat treatment

In the temperature range of $(293 \div 473)$ K, the obtained results indicate the formation of microregions with topological short-range order of α-Fe type in the investigated amorphous alloy $Fe_{78.5}Ni_{1.0}Mo_{0.5}Si_{6.0}B_{14.0}$. During heating to $T = 473$ K, the position of the main maximum of the curve $I(s)$ is slightly shifted toward larger values of s due to the topological ordering of the amorphous phase (Fig. 1). There is a decrease in the mean interatomic distance (r_1) due to the release of free volume during the structural relaxing of the amorphous alloy $Fe_{78.5}Ni_{1.0}Mo_{0.5}Si_{6.0}B_{14.0}$. It should be noted that upon heating above $T = 573$ K, there is an increase in the mean interatomic distance r_1 due to the decay of the amorphous phase in alloy $Fe_{78.5}Ni_{1.0}Mo_{0.5}Si_{6.0}B_{14.0}$ and formation of a microhomogeneous structure, whose the elements of which are nanoclusters based on α-Fe and $(Fe_3B)_T$ [4].

$a(S)$			$\Delta a(S)$	
T, K	293	77		
$Fe_{78.5}Ni_{1.0}Mo_{0.5}Si_{6.0}B_{14.0}$ (AMA-2)				
$a(S_1)$	3.146	3.202	$\Delta a(S_1)$	+0.056
$a(S_2)$	1.524	1.491	$\Delta a(S_2)$	−0.033
$a(S_3)$	1.052	1.019	$\Delta a(S_3)$	−0.033
$Fe_{73.1}Cu_{1.0}Nb_{3.0}Si_{15.5}B_{7.4}$ (AMA-3)				
$a(S_1)$	3.895	3.700	$\Delta a(S_1)$	−0.195
$a(S_2)$	1.530	1.573	$\Delta a(S_2)$	+0.043
$a(S_3)$	1.172	1.208	$\Delta a(S_3)$	+0.036
$Fe_{51.7}Ni_{21.7}Cr_{6.2}Mo_{0.6}V_{1.5}Si_{5.2}B_{13.1}$ (AMA-4)				
$a(S_1)$	3.799	3.731	$\Delta a(S_1)$	−0.068
$a(S_2)$	1.657	1.683	$\Delta a(S_2)$	+0.026
$a(S_3)$	1.222	1.318	$\Delta a(S_3)$	+0.096

Table 2. Structural factors [peak heights of diffractograms $a(S)$] of amorphous alloys based on Fe before and after cooling during 3 hours at $T = 77$ K

Alloy	Heating temperature, K	Element						
		Fe	Ni	Mo	Cu	Nb	Cr	V
AMA–2	293	92.95	1.30	1.49	—	—	—	—
	493	91.51	1.62	0.85	—	—	—	—
	77	92.87	1.10	1.20	—	—	—	—
AMA–3	293	84.41	—	—	1.47	7.03	—	—
	77	86.45	—	—	1.74	7.11	—	—
AMA–4	293	56.40	29,60	0.57	—	—	7.15	1.94
	77	58.30	29.70	0.26	—	—	7.53	2.12

Table 3. Elemental composition of AMA (wt.%) before and after heat treatment

The content of metallic elements in the AMA before and after the heat treatment was determined using energy-dispersion microanalysis (Table 3). When heated to 77 and 473 K, the content of Fe and Mo in AMA-2, decreased slightly, which is explained by the partial yield of Si to the surface and the volatility of molybdenum oxides [17]. For AMA-3 and AMA-4 at 77 K, the content of Fe, Cu, Nb and Ni, Cr, V, respectively, increased. Cooling of the alloy is accompanied by dissociative adsorption of water from the residual atmosphere with the formation of surface hydroxides [18].

It is important to assess the strength of amorphous materials, especially under the influence of low temperatures. Figure 2 shows the surface hardening coefficients calculated from the ratio of the microhardness values of the cooled samples to the microhardness of the initial amorphous alloys. AMA-2 was the least sensitive to cooling. One-hour exposure to $T = 77$ K strengthened the surface of AMA-3 most significantly, while for multicomponent AMA-4 one- and three-hour exposure reduced the strength of the alloy surface. Fluctuations in the hardening coefficients of the investigated amorphous alloys in the vicinity of the unit demonstrate the high mechanical stability of the AMA's surface.

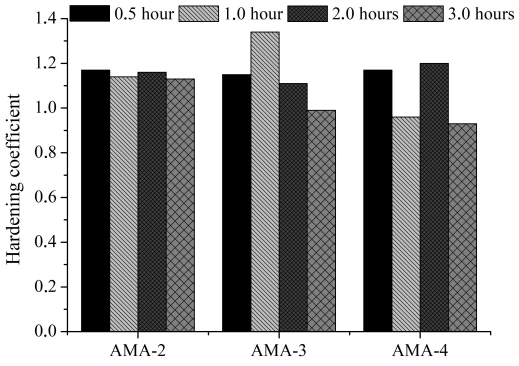

Fig. 2. Histogram of AMA surface hardening coefficients after treatment at $T = 77$ K for $(0.5 \div 3.0)$ h

Even insignificant changes in the structure and elemental composition of amorphous alloys affect their electrochemical characteristics, which is important in the practical use of AMAs as precision materials in aggressive environments. Due to the increase in the pre-treatment temperature of AMA $Fe_{73.1}Cu_{1.0}Nb_{3.0}Si_{15.5}B_{7.4}$ to 473 K, the values of the

surface potential after 20 min (E_f) become more positive compared to the initial E_0 (Table 4), the dissolution resistance of external and contact surfaces of the tape increases. In the presence of Ni and Mo in the $Fe_{78.5}Ni_{1.0}Mo_{0.5}Si_{6.0}B_{14.0}$ alloy we observe a decrease in the dissolution resistance due to the defects of oxide protective coatings because of the Mo oxides volatility. Additions of Cu and Nb in the alloy after the heat treatment at 473 K cause a significant acceleration of the surface redox processes stabilization, which is associated with active nanocrystallization [19] and high oxidizing ability of copper [20].

Low-temperature treatment of amorphous Fe-based alloys has different effects on their electrochemical parameters in the 0.5 M NaCl aqueous solution (Fig. 3). The $Fe_{80}Si_6B_{14}$ alloy proved to be the most resistant to low-temperature treatment. The corrosion resistance of alloys $Fe_{78.5}Ni_{1.0}Mo_{0.5}Si_{6.0}B_{14.0}$ and $Fe_{73.1}Cu_{1.0}Nb_{3.0}Si_{15.5}B_{7.4}$ decreases, while that of $Fe_{51.7}Ni_{21.7}Cr_{6.2}Mo_{0.6}V_{1.5}Si_{5.2}B_{13.1}$ increases.

In an aggressive aqueous environment, the surface of Fe-based AMA is easily covered with oxide-hydroxide layers, which resist active surface dissolution. The method of electrochemical impedance spectroscopy allows one to measure the resistance of oxide coatings to the transport of water molecules, oxygen, and ions to the metal surface. Analysis of the dependences of AMA $Fe_{78.5}Ni_{1.0}Mo_{0.5}Si_{6.0}B_{14.0}$ in 0.5 M NaCl aqueous solution (Fig. 4, Table 5) shows that the nature of the oxide film on both surfaces of the tape differs significantly. In the frequency range $(10^1 \div 10^5)$ Hz, on the Bode curves there is a section describing the electrolyte resistance (Fig. 4,a). In the frequency range $(10^{-1} \div 10^1)$ Hz, an increase in impedance is recorded — this area reflects the capacitive characteristics of the surface layers. In the lower frequency range, the frequency-independent area corresponding to the sum of the electrolyte resistance (R_1) and the film resistance (R_2) is fixed [21].

The resistance (R_2) of the surface oxide film of the AMA $Fe_{78.5}Ni_{1.0}Mo_{0.5}Si_{6.0}B_{14.0}$ contact surface is much lower than the external one, and the roughness (R_f) is higher. The oxide layer on such a surface will also be uneven and its protective properties may be low. As the temperature increases, the resistance R_2 increases due to the proximity to the beginning of the nucleation of nanocrystallization centers and compaction of the protective layers under the influence of heat treatment.

Similar investigations of cooled (T = 77 K) AMA based on Fe in an aggressive medium of 0.5 M NaCl (Table 6) showed that in this solution the most stable is an alloy doped with Cu and Nb, which, thanks to such additions, form dense oxide–hydroxide layers and alloy $Fe_{51.7}Ni_{21.7}Cr_{6.2}Mo_{0.6}V_{1.5}Si_{5.2}B_{13.1}$, were the addition of Cr improves the protective properties of surface films.

T, K	Surface	$Fe_{78.5}Ni_{1.0}Mo_{0.5}Si_{6.0}B_{14.0}$		$Fe_{73.1}Cu_{1.0}Nb_{3.0}Si_{15.5}B_{7.4}$	
		$-E_0$, V	$-E_f$, V	$-E_0$, V	$-E_f$, V
–	c	0.52	0.62	0.43	0.44
	e	0.50	0.66	0.33	0.42
373	c	0.46	0.63	0.41	0.48
	e	0.52	0.72	0.42	0.48
473	c	0.49	0.68	0.24	0.36
	e	0.45	0.73	0.21	0.35

Table 4. Chronopotentiometric investigation of the AMA electrodes oxidation in the 0.5 M NaCl aqueous solution after one hour heat treatment

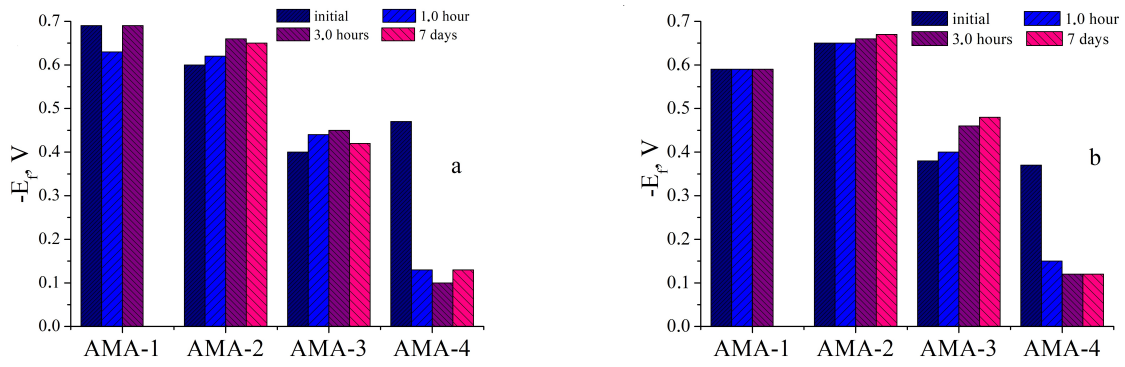

Fig. 3. Potentials of the contact (a) and external (b) surfaces of the initial and cooled samples of AMA based on Fe in the 0.5 M NaCl solution

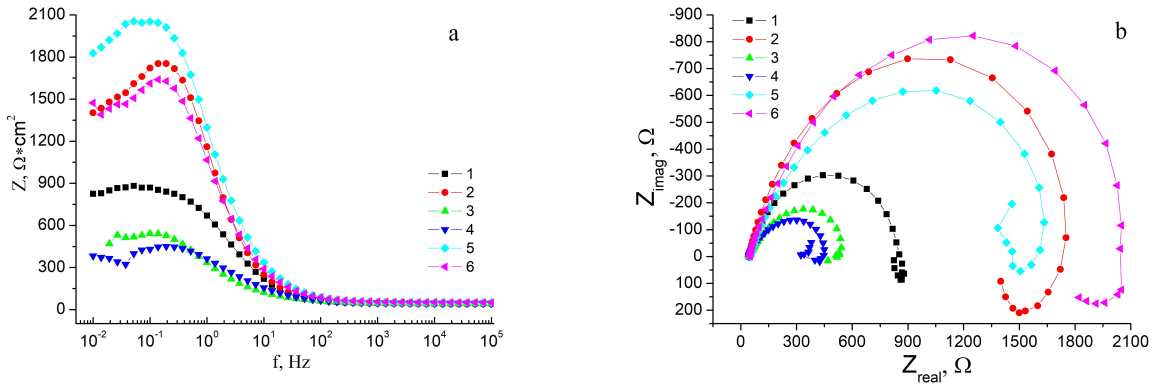

Fig. 4. Dependence of the impedance modulus on the current frequency (a) and Nyquist curves (b) in 0.5 M aqueous solutions of NaCl for the contact (1, 3, 5) and external (2, 4, 6) surfaces of the initial AMA $Fe_{78.5}Ni_{1.0}Mo_{0.5}Si_{6.0}B_{14.0}$ (1, 2) and after the heat treatment at 373 K (3, 4) and 473 K (5, 6)

T,K	Surface	R_1, Ω	E, V	R_2, Ω	$Q_{\text{dl}} \cdot 10^4$, F · cm^{-2}	α	R_{f}
293	c	44.47	−0.68	834.1	1.68	0.80	0.84
	e	41.08	−0.68	1873	1.32	0.82	0.66
373	c	43.24	−0.68	609.7	6.74	0.64	3.37
	e	43.92	−0,66	439.8	3.83	0.69	1.92
473	c	50.88	−0.66	1767	1.52	0.75	0.76
	e	49.66	−0.67	2251	1.24	0.77	0.62

Table 5. EIS parameters in the 0.5 M NaCl aqueous solutions for AMA $Fe_{78.5}Ni_{1.0}Mo_{0.5}Si_{6.0}B_{14.0}$ after the previous one-hour heat treatment

Cooling duration	Surface	R_1, Ω	R_2, Ω	$Q_{\text{dl}} \cdot 10^4$, F · cm^{-2}	α
$Fe_{80}Si_6B_{14}$					
—	c	11.12	886	1.97	0.85
	e	14.57	253	0.93	0.82
3 h	c	16.37	650	3.08	0.81
	e	12.85	940	1.45	0.80
$Fe_{78.5}Ni_{1.0}Mo_{0.5}Si_{6.0}B_{14.0}$					
—	c	13.15	1083	2.27	0.82
	e	15.07	378	1.03	0.81
3 h	c	13.87	752	3.24	0.82
	e	14.79	958	1.45	0.80
$Fe_{73.1}Cu_{1.0}Nb_{3.0}Si_{15.5}B_{7.4}$					
—	c	23.90	3432	0.20	0.86
	e	23.74	4893	0.14	0.87
3 h	c	21.61	2395	0.26	0.86
	e	24.65	6634	0.78	0.88
$Fe_{51.7}Ni_{21.7}Cr_{6.2}Mo_{0.6}V_{1.5}Si_{5.2}B_{13.1}$					
—	c	13.67	38515	0.19	0.88
	e	13.90	250830	0.08	0.90
3 h	c	12.91	129110	0.12	0.90
	e	14.62	308000	0.12	0.91

Table 6. Parameters of electrochemical impedance spectroscopy in the 0.5 M NaCl aqueous solution of the initial and cooled at $T = 77$ K amorphous alloys

IV. CONCLUSIONS

After the low-temperature treatment of AMA samples system Fe–Si–B–(Me), there were no significant changes in the structure, which indicates the durability of such materials to withstand heat treatment at 77 K. In the temperature range of (293 ÷ 473) K, the formation of a microhomogeneous structure, whose the elements are nanoclusters based on α-Fe and $(Fe_3B)_T$ was recorded for Fe-based amorphous alloys.

Fluctuations in the hardening coefficients of the investigated amorphous alloys in the vicinity of the unit demonstrated the high mechanical stability of the AMA's surface at 77 K.

As the temperature increases, the resistance in the 0.5 M NaCl solution of Fe-based alloys increases due to the proximity to the beginning of the nucleation of nanocrystallization centers and compaction of the protective layers under the influence of heat treatment. Similar investigations of cooled AMA based on Fe in the aggressive medium of 0.5 M NaCl showed that in this solution the most stable is the alloy $Fe_{73.1}Cu_{1.0}Nb_{3.0}Si_{15.5}B_{7.4}$.

[1] S. I. Mudry, Yu. S. Nykyruy, Chem. Met. Alloys **4**, 85 (2011); https://doi.org/10.30970/cma4.0167.

[2] M.-O. M. Danylyak, L. M. Boichyshyn, Mat. Sci. **55**, 921 (2020); https://doi.org/10.1007/s11003-020-00388-z.

[3] D. T. H. Gam, N. D. The, N. H. Hai, J. Korean Phys. Soc. **52**, 1423 (2008).

[4] O. M. Hertsyk, T. H. Pereverzeva, L. M. Boichyshyn, M. O. Kovbuz, N. L. Pandyak, Mat. Sci. **54**, 526 (2019); https://doi.org/10.1007/s11003-019-00213-2.

[5] E. Jakubczyk, L. Krajczyk, P. Siemion, M. Jakubczyk, Opt. Appl. **37**, 359 (2007).

[6] T. Kulik, J. Non-Cryst. Solids **287**, 145 (2001); https://doi.org/10.1016/S0022-3093(01)00627-5.

[7] L. Bednarska, *et al.*, J. Non-Cryst. Solids **354**, 4359 (2008); https://doi.org/10.1016/j.jnoncrysol.2008.06.051.

[8] S. Guo, Y. Liu, J. Non-Cryst. Solids **358**, 2753 (2012); https://doi.org/10.1016/j.jnoncrysol.2012.06.023.

[9] D. G. Onn, J. Appl. Phys. **52**, 1788 (1981); https://doi.org/10.1063/1.329715.

[10] G. Rajaram, IEEE Trans. Magn. **20**, 1347 (1984); https://doi.org/10.1109/TMAG.1984.1063537.

[11] M. Lopachak *et al.*, in *Proceedings of the 2020 IEEE 10th International Conference on Nanomaterials: Applications and Properties*, 9309640 (2020); https://doi.org/10.1109/NAP51477.2020.9309640.

[12] L. Boichyshyn, M. Kovbuz, O. Hertsyk, V. Nosenko, B. Kotur, Phys. Sol. State. **55**, 243 (2013); https://doi.org/10.1134/S1063783413020054.

[13] Materials science in mechanical engineering, http://www.znanius.com/1963.html.

[14] M.-O. M. Danyliak, L. M. Boichyshyn, N. L. Pandiak, Acta Phys. Pol. A **133**, 1103 (2018); https://doi.org/10.12693/APhysPolA.133.1103.

[15] L. M. Bednars'ka, O. M. Hertsyk, O. B. Danylyuk, O. A. Ezers'ka, V. K. Nosenko, Mat. Sci. **40**, 113 (2004); https://doi.org/10.1023/B:MASC.0000042793.62972.f7.

[16] O. M. Hertsyk, M. O. Kovbuz, T. H. Pereverzeva, A. K. Borysyuk, L. M. Boichyshyn, Mat. Sci. **50**, 454 (2014); https://doi.org/10.1007/s11003-014-9742-3.

[17] L. M. Bednars'ka, O. M. Hertsyk, M. O. Kovbuz, Mat. Sci. **41**, 653 (2005); https://doi.org/10.1007/s11003-006-0027-3.

[18] O. M. Hertsyk, M. A. Kovbuz, T. G. Pereverzeva, L. M. Boichyshyn, B. Ya. Kotur, Russ. J. Appl. Chem. **86**, 802 (2013); https://doi.org/10.1134/S1070427213060025.

[19] L. Bednarska, G. Haneczok, M. Kovbuz, B. Kotur, O. Hertsyk. Mat. Sci. **43**, 890 (2007); https://doi.org/10.1007/s11003-008-9036-8.

[20] J. E. May, P. A. Nascente, S. E. Kuri, Corros. Sci. **48**, 1721 (2006); https://doi.org/10.1016/j.corsci.2005.05.024.

[21] O. M. Hertsyk, M. O. Kovbuz, O. A. Ezers'ka, T. H. Pereverzeva, Mat. Sci. **47**, 401 (2011); https://doi.org/10.1007/s11003-011-9409-2.

ВПЛИВ ТЕМПЕРАТУРНОЇ МОДИФІКАЦІЇ НА ВЛАСТИВОСТІ АМОРФНИХ СПЛАВІВ НА ОСНОВІ Fe

О. М. Герцик[1], Т. Г. Гула[1], М. О. Ковбуз[1], О. А. Єзерська[2], Ю. О. Кулик[1], Н. Л. Пандяк[3]

[1] *Львівський національний університет імені Івана Франка, вул. Кирила і Мефодія, 6, Львів, 79005, Україна,*

[2] *Інститут технології виробництва та передових матеріалів Фраунгофера, вул. Віденська, 12, Бремен, 28359, Німеччина,*

[3] *Національний лісотехнічний університет України, вул. Ген. Чупринки, 103, Львів, 79057, Україна*

Досліджено вплив температурної модифікації за $T = 77$ K протягом 0.5, 1.0, 2.0, 3.0 годин і 7 днів та в температурних межах (273 ÷ 673) K протягом 1 години на фізико-хімічні властивості аморфних сплавів $Fe_{80}Si_6B_{14}$, $Fe_{78.5}Ni_{1.0}Mo_{0.5}Si_{6,0}B_{14.0}$, $Fe_{73.1}Cu_{1.0}Nb_{3.0}Si_{15.5}B_{7.4}$, $Fe_{51.7}Ni_{21.7}Cr_{6.2}Mo_{0.6}V_{1.5}Si_{5.2}B_{13.1}$.

Після температурної обробки аморфних сплавів були зафіксовані незначні зміни в структурі, елементному складі поверхні й мікротвердості досліджуваних матеріалів. Електрохімічні характеристики зразків у 0.5 М водному розчині NaCl також були оцінені. Найнижчу корозійну стійкість у такому розчині продемонстрував сплав $Fe_{80}Si_6B_{14}$, а найвищу — $Fe_{51.7}Ni_{21.7}Cr_{6.2}Mo_{0.6}V_{1.5}Si_{5.2}B_{13.1}$. Поверхневі захисні шари, що формуються на багатокомпонентному сплаві, мають найкращі захисні властивості.

Ключові слова: аморфні металеві сплави, температурна модифікація, структурні характеристики, електрохімічні властивості.